Comparison of predicted and measured pile driving processes at steel pipe piles in North and Baltic Seas

Peer Kortsch [i)] and Fabian Kirsch [i)]

i) GuD Geotechnik und Dynamik Consult GmbH, Darwinstraße 13, 10589 Berlin, Germany.

ABSTRACT

Foundation types of offshore wind turbines are mainly realised with steel pipe piles whereas most commonly monopiles with large diameters or jacket piles are used. Against the background of cost effectiveness, the selection of a driving system as well as design fatigue calculations it is of major importance to run driveability analyses prior to the installation process. Essential criteria for that are the duration of a driving process and number of blows, pile driving stresses in compression and tension and soil resistance to driving (SRD). While the application of SRD models for impact driven piles in sand and clay is considered as well established a trusted prognosis of pile driving in other soils or materials like chalk or the prognosis of vibratory pile driving is still a challenge.
At real pile driving usually dynamic pile driving monitoring is performed in order to record real blow counts and stresses in the pile and furthermore, to verify pile capacity. In this paper driveability analyses and SRD models are compared with results of dynamic pile tests and pile driving monitoring in selected offshore wind farm projects in the North and Baltic Seas in order to check their applicability. Measurements were taken during the pile driving of small and large diameter pipe piles in sand or chalk dominated soils by the use of impact and, partly, vibratory hammers. Using appropriate wave equation software (GRLWEAP) driving processes could be recalculated and compared to measured data and records of the driving system.

Keywords: impact and vibratory driveability, pile driving monitoring, SRD, wave equation analysis

1 INTRODUCTION

Prior to installation works simulations of pile driving are reasonable to determine suitability of certain driving systems in terms of a safe installation connected to recommendations for system parameters (e.g. weight and stroke of impact hammer, eccentric moment and frequency of vibratory hammer). The goal is to optimise the driving progress (blow count, penetration speed) while reducing pile stresses. The latter will be used as input parameters for analysing driving fatigue in steel construction.

A main aspect for driveability is the knowledge of soil resistances at shaft and toe (Static Resistance to Driving SRD). In general, soil behave differently during dynamic excitation due to changes in friction and pore pressure as on static almost constant loads. Static resistances will be initially reduced and set up after a certain waiting time depending on soil types occures. In literature (e.g. (Chow et al., 1998), (Skov et al., 1988)), one finds examples for quantification of those effects.

Common methods for estimating SRD in granular and cohesive soils are presented e.g. by (Alm & Hamre, 2001) with averaging after (Schneider & Harmon, 2002) and Stevens et al. (1982). Recently, (Jardine et al., 2018), (Buckley et al., 2019) and (Buckley et al., 2020) presented a model for SRD calculation in chalk as met in Baltic Sea area. All the above is connected to impact driving.

Static resistance to vibratory driving was investigated for instance by (Huybrechts et al., 2002) and (Holeyman and Whenham, 2017) leading to the Hypervib I model amongst others.

Estimated soil resistances will be used as input parameters for simulation software GRLWEAP in order to analyse the dynamic driving process for a given hammer or vibrator and pile/soil-system (GRL Engineers, 2008)).

Present paper deals with a comparison of specific SRD methods in relation to corresponding, real measurement data at offshore wind farms. With the help of those

examples taken from own data base the applicability of used SRD methods will be shown.

2 STATIC RESISTANCE TO DRIVING (SRD)

To address the effect of reduction in static soil resistances due to pile driving shaft friction Q_s and end bearing Q_b are to be chosen whereas the total resistance Q_{SRD} ([kN]) is the sum of resistances at shaft and toe (e.g. see (API, 2000):

$$Q_{SRD} = Q_S + Q_b = fA_s + qA_b \quad (1)$$

Terms fA_s und qA_b represent the products of shaft friction (summation over particular pile penetration levels) and end bearing with corresponding areas, respectively. Depending on whether to expect plugging or non-plugging situations inside an open-ended steel pipe during installation the SRD calculation differs in terms of specifying toe area as being a full circle or pile annulus ring. Equation (1) will be modified to:

- Plug: $Q_{SRD} = Q_{S,outside} + Q_{end}$ (2a)
- No plug: $Q_{SRD} = Q_{S,outside} + Q_{S,inside} + Q_{ann}$ (2b)

with

$Q_{s,\,außen}$: Outer shaft resistance,
$Q_{s,\,innen}$: Inner shaft resistance,
Q_{end}: Toe resistance, full circle,
Q_{ann}: Toe resistance, pile annulus.

Particularly during offshore installations, where open ended steel pipe piles with diameters often larger than 8 m (Monopiles) are used sufficient inner friction and complete emergence of a plug are not to be expected (Rausche et al, 2011)). It can rather be assumed that soil will further penetrate into the pipe (coring). Here, shaft friction forces act both outside and inside the pile. Toe resistance take only effect at pile annulus.

2.1 Loose and solid rocks – Impact driving

All presented SRD models base upon the above-mentioned approach. Hereafter, two typical models for granular soils are presented that have been used in the present study to compare results of real driving processes with driveability analyses:

A. Method of (Alm & Hamre, 2001) with averaging after (Schneider & Harmon, 2002),
B. Method of (Stevens et al., 1982) with regard to (API, 2000).

Essential input parameters are taken from design soil profiles (friction angle, cohesion, specific weight). Furthermore, in method A cone penetration test (CPT) data will be used.

The method of (Alm and Hamre, 2001) was developed on the basis of extensive measuring data of impact driven piles (Diameter: 1.8 till 2.7 m, Installation depth: down to 90 m) in the North Sea. Impact hammers were IHC S-400 and S-2300 as well as Menck MHU 1000 till 3000.

To estimate shaft friction between pile and surrounding soil (SRD) the following basic formulas was developed:

$$f = f_{sres} + (f_{si} - f_{sres}) \cdot e^{k(d-p)} \quad (3)$$

with

f, f_{si}, f_{sres} Shaft friction [kN/m²] (total, initial and residual),
d Depth of soil element [m],
p Pile tip penetration [m],
k Shape factor for degradation = $(q_t/p_0')^{0,5}/80$ [-],
q_t Total cone tip resistance from CPT [kN/m²],
p_0' Effective overburden pressure [kN/m²].

Depending on the type of soil, sand or clay, (Alm and Hamre, 2001) have derived different approaches for f_{si} and f_{sres}.

The method considers a degradation of shaft friction along the pile shaft while pile driving goes on to further depths ('friction fatigue'). It is accounted for in equation (3) by the means of the exponential decay. This term includes the relation between q_t and p_0' whereas in dense sand a faster degradation occurs than it does in soft clay (Alm and Hamre (2001)). This model was evaluated in (Meynard et al., 2019) with the outcome that it fits reasonably well in sand and clay comparable to the material where the method was initially calibrated.

When the pile toe meets a soil element in a certain installation depth the shaft friction f_s amounts to initial value f_{si} firstly and converges to residual value f_{res} with increasing pile penetration. The implementation of this multidimensional equation into software package GRLWEAP (GRL Engineers, 2010) is not readily possible. (Schneider and Harmon, 2010) present an averaging method where a pseudo average incremental shaft friction Δf_{avg} of consecutive SRD calculations is determined to serve as input data:

$$\Delta f_{avg} = \frac{\sum Q_{S,L} - \sum Q_{S,L-1}}{\pi D \cdot \Delta L} \quad (4)$$

with

$\Sigma Q_{S,L}$ Cumulative shaft resistance at the pile tip depth of current SRD calculation [kN],
$\Sigma Q_{S,L-1}$ Cumulative shaft resistance at the depth of the previous SRD calculation [kN],
ΔL Length of the pile between $\Sigma Q_{S,L}$ und $\Sigma Q_{S,L-1}$ [m],
D Pile diameter [m].

(Alm and Hamre, 2001) suggests to implement a "Best Estimate" for total resistance based on equation (3) and an "Upper bound". The latter is calculated by the application of a factor 1.25 upon "Best estimate" values in order to take local soil variability and corresponding parameters into account.

In comparison to real measuring data taken from impact driving of piped piles (Diameters: 0.90 till 1.05 m) in the Arabian Gulf researcher team of (Stevens et al., 1982) have performed driveability analyses. Their model corresponds mainly to recommendations of (API, 2001) for pile bearing capacity determination.

Input parameters are solely geotechnical parameters no CPT data are used.

To derive skin friction f and end bearing q_t following formulas were taken from (Stevens et al., 1982) and (API, 2000) in case of cohesive and granular soils:

- Cohesive soils: $f_{Clay} = \alpha c$ (5a)

$q_{t,Clay} = 9c$ (5b)

- Granular soils: $f_{Sand} = K p_0' (tan\,\delta)$ (5c)

$q_{t,Sand} = p_0' N_q$ (5d)

with

α dimensionless factor, (API, 2000),
c undrained shear strength [kN/m²],
K dimensionless coefficient of lateral earth pressure (K = 0,7…0,8) (Stevens et al, 1982 and API, 2000),
p_0' effective overburden pressure [kN/m²],
δ angle of friction between pile and soil,
N_q dimensionless bearing capacity factor (between 8 and 50, (API, 2000).

Upper limits for f and q are taken from (API, 2000) when encountering cohesionless soils (see Table 1).

Table 1. Limiting values for cohesionless soils, after API (2000).

Density	Soil	Limiting Unit Skin Friction [kPa]	Limiting Unit End Bearing [MPa]
Very Loose Loose Medium	Sand Sand-Silt Silt	47.8	1.9
Loose Medium Dense	Sand Sand-Silt Silt	67.0	2.9
Medium Dense	Sand Sand-Silt	81.3	4.8
Dense Very Dense	Sand Sand-Silt	95.7	9.6
Dense Very Dense	Gravel Sand	114.8	12.0

(Stevens et al., 1982) consider "lower bound" and "upper bound" soil resistance values including or excluding plugged situations.

2.2 Variable solid rocks (chalk) – Impact driving

Prognosis of SRD values for variable solid rocks is a specific challenge. Encouraged by recent investigations described in (Jardine et al., 2018), (Buckley et al., 2019) and (Buckley et al., 2020) within campaigns conducted onshore and offshore in the North West Baltic Sea their ICP-18 method predicting SRD in chalk is applied to own measurement datasets. (Buckley et al., 2019) have shown that effective stress states are key aspects which are changing in the course of the driving process.

The following equations were found:

$$\tau_{rzi} = \sigma'_{ri} * \tan(\delta'_{ult}) \quad (6a)$$

$$\sigma'_{ri} = 0{,}031 * q_t \left(h/_{R^*}\right)^{-0.481\left(\frac{D}{t_w}\right)^{0.145}} \quad (6b)$$

with

τ_{rzi} short term shaft resistance at EOD [kN/m²],
σ'_{ri} radial effective stress during driving [kN/m²],
δ'_{ult} ultimate interface angle of shearing resistance,
t_w D wall thickness and pile diameter [m],
q_t net cone resistance averaged over 300 mm [kN/m²].
$h/_{R*}$ Ratio between distance to pile tip h and equivalent radius R^* (= $R^2_{outer} - R^2_{inner}$) .

Relative rates of degradation with h/R* are far larger in chalk than in sand or clays according to (Buckley et al., 2020). Furthermore, their datasets delivered values of pile end bearing resistances of 0.4…0.6 times $q_{t1,5D}$. Ratios of D/t_W in the range of 16 to 67 were used. Values of δ'_{ult} had been measured via interface ring shear tests and covered 30.5 to 32 degrees.

2.3 Soils – Vibratory driving

The determination of soil resistance during vibratory driving is a key parameter but not as well investigated as it is for impact driving. In general, surrounding subsoil acts differently during vibratory pile driving compared to static loading or impact driving. Soil models base on the assumption that in cohesionless soils under extreme conditions liquefaction due to cyclic load may occur (see (Huybrechts et al., 2002), (Holeyman and Whenham, 2017). (Massarsch et al., 2017) stated that the vertically oscillating force generated by the vibrator creates a horizontal component in the soil which is directed away from the pile and reduces shear resistances with ongoing downward movement. This is believed to be the main reason for good applicability in coarse grained soils. In cohesive soils the magnitude of the eccentric moment of the vibrator is important for the vibratory driving as it determines the relative displacement between pile and soil (Massarsch et al., 2017).

(Huybrechts et al., 2002) have investigated in detail vibratory pile driving processes and derived a CPT based method for defining the soil driving resistance due to vibratory driving. Later on, this so-called Hypervib I model was updated (see Holeyman and Whenham, 2017). (Viking, 2002) refers to that within a detailed investigation campaign including field data recalculations at sheet piles.

Static base and shaft resistances are derived directly from CPT results as the first step whereas (Viking, 2002) suggested an evaluation in averaging the data inside defined zones I, II and III above and below pile toe as follows:

$$q_S = 1/2\ (I + II) \quad (7a)$$

$$f_S = 1/2\ (2III) \quad (7b)$$

with

I	Averaging between the level of the base and a distance (I=b/4) above the base,
II	Averaging between the level of the base and a distance (II=3b/4),
III	Averaging between the level of the sleeve and an equal distance (III=b/2) below an above the sleeve,
b	Width of the sheet pile.

Secondly, a liquefied resistance is estimated based on an exponential law with the use of specific factors and the given values of step one. The third step was to derive the driving base and shaft resistances from the static and liquefied modes.

Herein, it is assumed that during vibratory driving a degradation of soil resistances over time occurs when the pile is driven along the certain soil elements. The driving resistance is a value in between the static and the liquefied states depending on vibratory hammer properties (acceleration amplitude of vibrating parts).

Basis formulas for liquefied resistances according to (Holeyman and Whenham, 2017) are:

$$q_l = q_s[(1 - {}^1/_L) * e^{-c_b/FR} + {}^1/_L] \quad (8a)$$

$$\tau_l = \tau_s[(1 - {}^1/_L) * e^{-c_s/FR} + {}^1/_L] \quad (8b)$$

Basis formulas for driving resistances are:

$$q_d = (q_s - q_l) * e^{-\alpha} + q_l \quad (9a)$$

$$\tau_d = (\tau_s - \tau_l) * e^{-\alpha} + \tau_l \quad (9b)$$

with

$\tau_l\ \tau_s\ \tau_d$	shaft resistances (liquefied, static and driving),
$q_l\ q_s\ q_d$	toe resistances (liquefied, static and driving),
FR	Friction ratio from CPT,
$c_S\ c_b$	empirical factors, defining the degradation level for shaft and base resistances,
L	Liquefaction factor (loss of resistance attributable to liquefaction, range: 8…10),
α	Acceleration ratio (a/g), when g is acceleration of gravity.

At each depth the vibratory pile driving resistance can be calculated as in equation (1) whereas no explicit distinction is made between inner and outer shaft friction. A more detailed description of the model as well as sensitivity studies can be found in (Holeyman and Whenham, 2017).

3 DATA ANALYSIS OF PILE DRIVING MEASUREMENTS

During impact driving of open-ended steel piles in the North and Baltic Sea dynamic pile driving monitoring was performed. The results shall serve as verification examples for the above described methods to predict pile driveability.

3.1 North Sea project – Impact driving

Steel pipe piles (diameter: 2.4 m, wall thickness variable) of North Sea project were driven with impact hammer IHC S-1200 starting from a penetration depth of about 10...13 m.

Soil structure was identified as sandy layers with enclosures of cohesive material. Figure 1 show results of CPT at locations A, B and C. While soil at location A is characterised by an alternating sand and clay sequence solely sand was found at locations B and C.

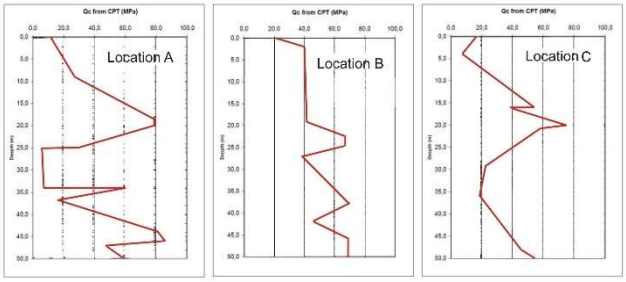

Fig. 1. CPT data at locations A, B and C, North Sea sand.

Before pile installation two strain gages and two accelerometers were attached to record each impact blow. Both sets of sensors (strain gage and accelerometer, respectively) were bolted at the pile shafts in 180° on opposite side a distance of 2.85 m below pile top. Wall thickness at this section was 50 mm as well as at pile toe.

Data acquisition was carried out with Pile Driving Analyser (PDA) from Pile Dynamics USA. Figure 2 show photographs of sensor application and pile driving.

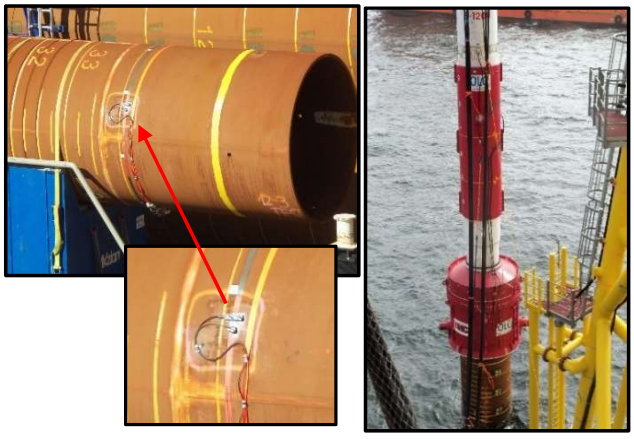

Fig. 2. Applied sensors at the test pile (left), pile driving (right).

Hammer log data and measuring data provided depth dependent information about blow count, energy just before impact as well as transferred energy to the pile, pile stresses and soil resistances SRD to be relevant for present data analyses.

Real pile driving and later driveability analyses were done by using hammer IHC S-1200 (IHC Hydrohammer, 2013). In Table 2 hammer parameters are listed.

Table 2. Hammer and test pile parameters, North Sea sand (IHC Hydrohammer, 2013).

Parameter	Dimension	IHC S-1200
Maximum Energy	[kJ]	Approx. 1.200
Weight of ram	[kN]	Approx. 600
Weight of anvil	[kN]	221
Maximum stroke	[m]	2.02
Stroke per blow	[m]	Calibrated at pile test data
Hammer efficiency	[%]	Calibrated at pile test data
Penetration at end of driving	[m]	33.60 - 35.50

3.2 Baltic Sea project – Impact driving

The installation of two axially loaded piles with a diameter D of 5 m and variable wall thickness into a chalk formation at Baltic Sea was accompanied by dynamic measurements. Here, a hammer of type IHC S-1800 was used. Sensor level was 7.25 m below pile top (wall thickness t at sensor level 85 mm, and at pile toe 80 mm). At pile toe this leads to a D/t ratio of 62.5. The soil mainly consists of a thick chalk formation starting at 24 m below sea floor and sand and till above it so that driving inside the chalk formation was of major importance. This was identified as being fine grained white lime stone with compression strengths in the wide range of 200 kN/m² till 2500 kN/m². Furthermore, it was characterized as being relatively soft, high in porosity and natural water content. After crushing a very soft consistency occurred. Parameters of pile driving and later simulations are listed in Table 3.

Table 3. Hammer and test pile parameters, Baltic Sea chalk (IHC Hydrohammer, 2013).

Parameter	Dimension	IHC S-1800
Maximum Energy	[kJ]	Approx. 1.800
Weight of ram	[kN]	Approx. 870
Weight of anvil	[kN]	1226
Maximum stroke	[m]	2.08
Stroke per blow	[m]	Calibrated at pile test data
Hammer efficiency	[%]	Calibrated at pile test data
Penetration at end of driving	[m]	65.10

3.3 North Sea project – Vibratory driving

The installation of large diameter steel pipe piles at an offshore wind farm in the North Sea shall be carried out by using a vibratory hammer of triple configuration (static moment of 1920 kgm).

The project is still in development at this stage and measuring data of real vibratory driving processes are not being gained yet.

4 COMPARISON BETWEEN MEASURING RESULTS AND DRIVEABILITY ANALYSES

4.1 Analysis model

Driveability analysis was performed with software package GRLWEAP, offshore version 2010 (GRL Engineers, 2010). Based on wave equation method the dynamic piling process will be simulated for a given hammer-pile-soil-system. Hammer and pile are modelled as a series of masses and springs. The soil is modelled with springs representing the static portion and damper elements for dynamic effects. Those are characterized with regard to quake as transition from elastic to plastic deformation and damping values relating the dynamic portion. This model was introduced by (Smith, 1960) and further developed (e.g. (Rausche et al., 2004).

Results of driveability are depth dependent developments of soil resistance (SRD) and blow count as well as compressive and tensile stresses.

Quake and damping values seen in Table 4 were chosen according to (GRL Engineers, 2010).

Table 4. Static and dynamic soil parameters for driveability (GRL Engineers, 2010).

	Pile shaft	Pile toe
Quake	2.54 mm	2.54 mm
Damping	0.16 s/m (sand)* 0.65 s/m (clay) 0.16 s/m (chalk)	0.49 s/m*
	* doubled for vibro driving	

Damping values in Table 4 are in accordance with common experiences of other authors (Soares et al., 1984).

While installing open-ended steel pipe piles offshore (Webster and Robinson, 2013) recommend higher values for the toe quake depending on pile diameters D (D/120 or sand, D/60 for clay). Since the pile shaft friction is of more importance than the end bearing at those situations the effect of having larger toe quakes plays a minor role in blow count estimation for sand/clay (Webster and Robinson, 2013).

4.2 Driveability and results in sandy and clayey soils, North Sea project – Impact driving

For present investigations with pile diameters of 2.40 m it was assumed that no plugging occurred during pile driving, but rather soil material cored into the pile with mobilising inner shaft friction.

Furthermore, no factorising of SRD values was considered for possible soil variabilities so that simulation calculations were run in the “Best Estimate” case of (Alm and Hamre, 2001) and “Lower Bound” no plug case of (Stevens et al., 1982). Calculation of skin friction of cohesive soils (equation 5a) was done

according to (API, 2000) without considering over consolidation ratio OCR.

Idealised red marked graphs of q_c in Figure 1 were used for SRD calculation. In Figures 3, 4 and 5 recorded hammer logs and gained measuring data of dynamic pile tests at locations A, B and C are opposed to theoretical results of comparative driveability in a more detailed form. This comprise depth dependent readings of energy (right before impact inside the hammer and transferred to pile), blow counts per 25 cm penetration, pile stresses in compression and tension as well as SRD values.

Soil resistances derived during measurements are based on CASE formula which only can serve as rough estimation regarding pile capacity including CASE damping values J_c. To indicate a band with J_c was chosen to 0.4, 0.6 and 0.8. More plausible damping values are generally achieved via CAPWAP analyses at which an advanced pile soil model will be established and system parameters (quake, damping) both for Smith model and corresponding CASE evaluation can be estimated iteratively. By doing CAPWAP analysis at one of the last blows of driving process corresponding CASE damping values of 0.5 - 0.6 could be found so that dark blue curves for $J_c = 0.4$ and $J_c = 0.6$ in Figures 3, 4 and 5 (below right) are relevant.

Main parameter to achieve a good fit between driveability and real driving processes was the adjustment of driveability calculated to measured transfer energy ENTHRU. The upper left diagram in Figures 3, 4 and 5 show measured energy via PDA near pile top as blue curves and calculated energy based on simulated calculations after (Alm and Hamre, 2001) and (Stevens et al., 1982) which are brought into overlay (green and violet curves).

In general, a discrepancy between those energies at pile head and the hammer registered energy right before impact (red curves) is observable leading to a reduction of about 77 % on average. This is due to energy loss in the transition zone between hammer/driving system and pile head - sensor level.

Overlapping energies of measuring data (PDA) with prognosis data (GRLWEAP) provide the basis for the following observations.

Diagrams in the upper right of Figures 3 till 5 show depth dependent blow count development per 25 cm penetration taken from measuring data (IHC-Hammer red line, PDA blue curve) and driveability calculations (green and violet curves).

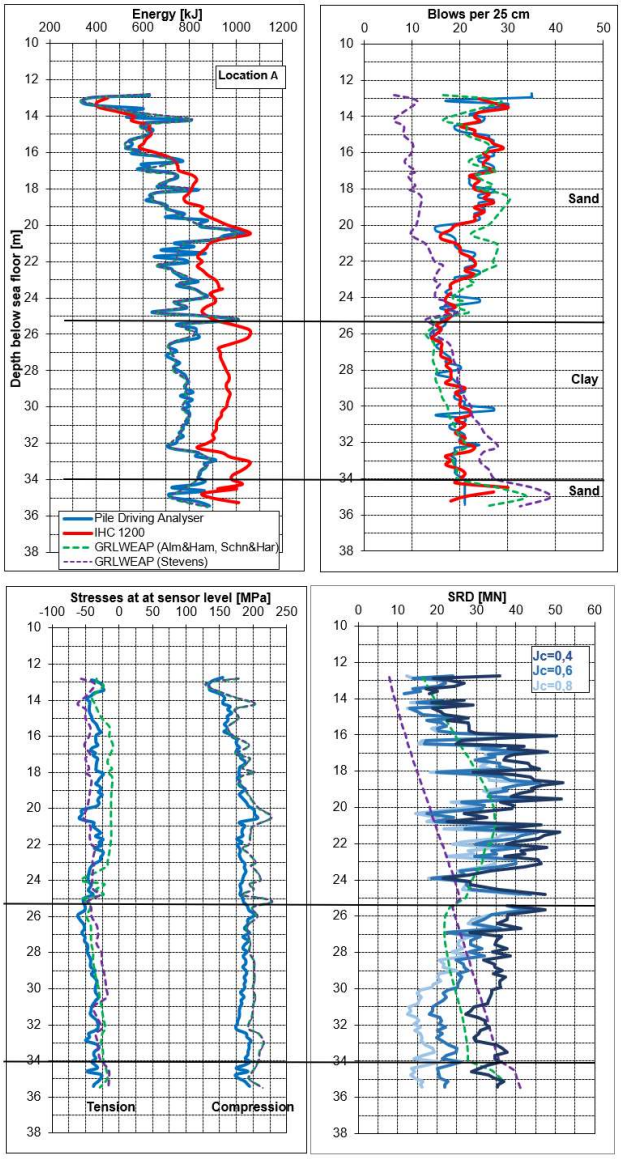

Fig. 3. Location A: Comparison of results from recorded hammer data, measuring data of dynamic pile test and driveability analyses (energy, blows per 25 cm penetration, pile stresses, SRD).

Applying method of (Alm and Hamre, 2001) with averaging after (Schneider and Harmon, 2010) a good agreement between theoretical blow counts and those from the field data can be found. This appears to be valid for both sand and clay layers. SRD method of Stevens et al. display lower blow counts at shorter penetrations down to approx. 20 m. Further down and at final penetration blow count based on Stevens et al.'s method led to a partly high overestimation.

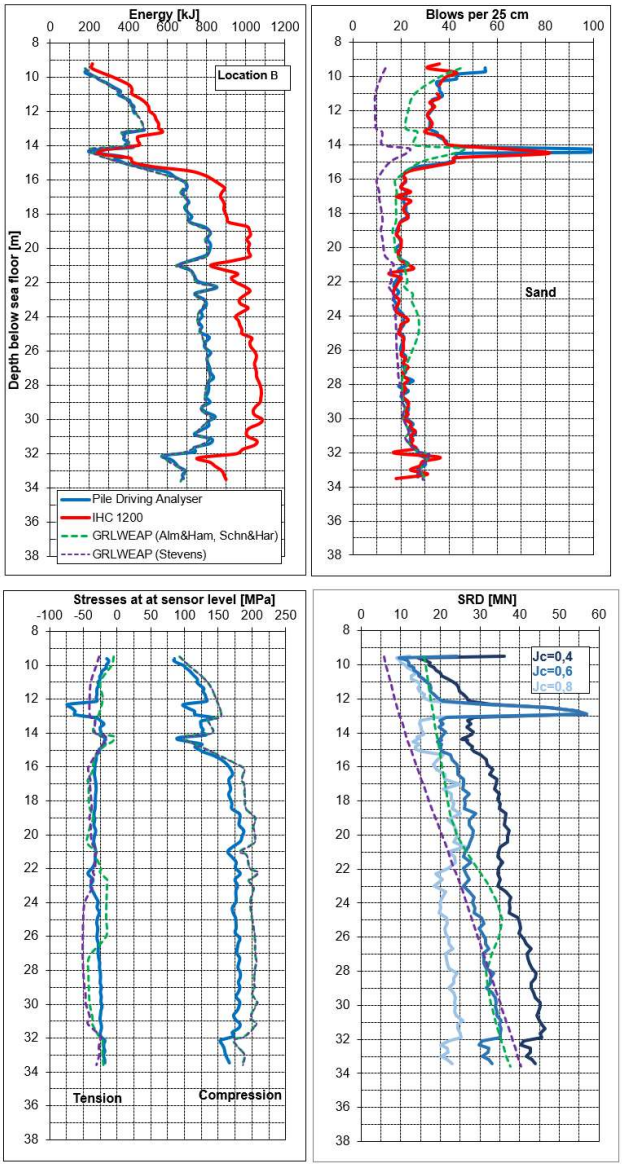

Fig. 4. Location B: Comparison of results from recorded hammer data, measuring data of dynamic pile test and driveability analyses (energy, blows per 25 cm penetration, pile stresses, SRD).

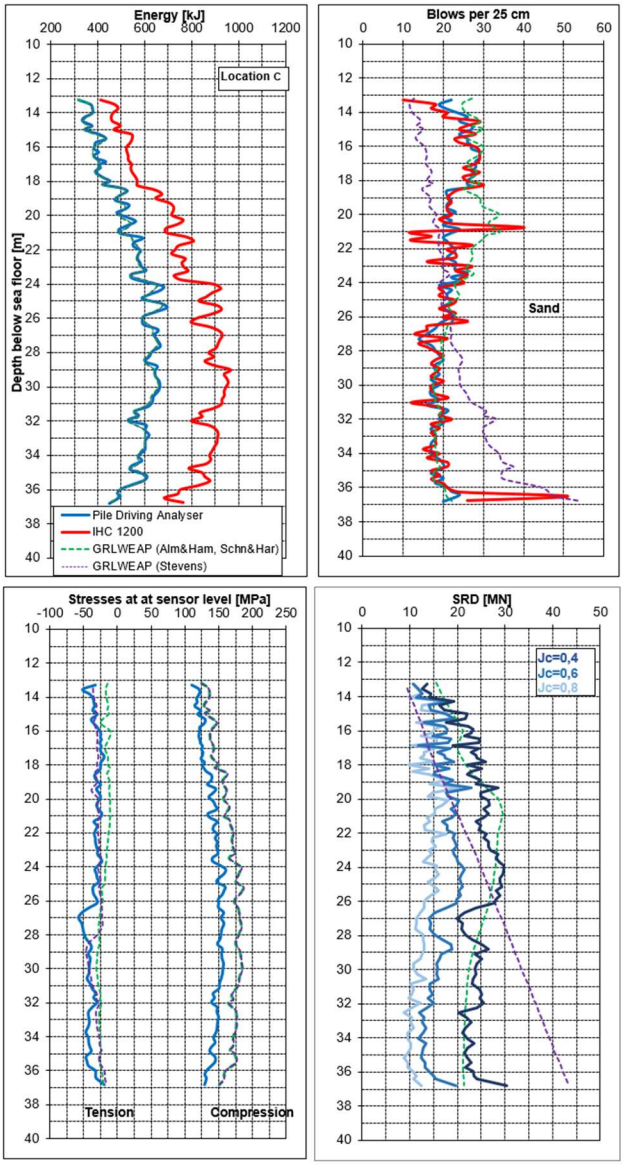

Fig. 5. Location C: Comparison of results from recorded hammer data, measuring data of dynamic pile test and driveability analyses (energy, blows per 25 cm penetration, pile stresses, SRD).

Comparison of pile stresses in compression and tension as well as total soil resistances (SRD) can be seen in the lower left and lower right graphs of Figures 3 till 5, respectively.

Theoretical tensile stresses are slightly lower than the measured values whereas a continuous "gap" is visible between compressive stresses taken from measurements and that from simulations. Comparative calculations led to higher stresses in compression so that a safe side can be assumed in terms of fatigue analyses since an absolute summation of compressive and tensile stresses was considered then.

Total resistance (SRD) show best agreement between measured and theoretical values by the use of (Alm and Hamre, 2001) method (see green and blue curves in Figures 3 till 5). There are lower SRD values at shorter penetration levels for Stevens' et al. method and an overestimation next to final penetration at location C and all methods reveal a slight reduction in SRD occurs as can be seen on the basis of the measuring data.

4.3 Driveability and results in variable solid rock (chalk), Baltic Sea project – Impact driving

A major drawback of all prediction methods is the difficulty to gain reliable CPT data for the massive chalk layer. Thus, in this project for determination q_c values an indirect method was chosen based on the following relation between uniaxial compression strength and cone penetration resistance:

$$q_u = q_c/32 \qquad (10)$$

Figure 6 shows the context. The trendline follows the finding that there is a distinction made between an upper chalk layer (about 25 m till 47 m) and a lower one (until final penetration depth of 65 m) in terms of its strength.

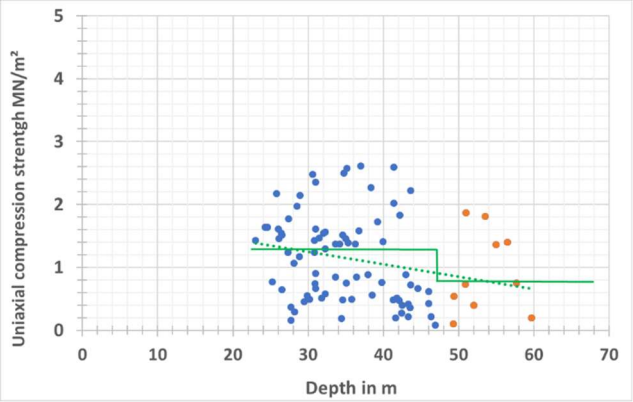

Fig. 6. Compression strength in chalk formation (blue dots: upper chalk layer, orange dots: lower chalk layer, dotted green: trend line and solid green: applied q_u values within the calculations).

Values of qc representing a rough estimation over the certain depth intervals were taken as 1200 kN/m² and 800 kN/m² (see Figure 6).

At the beginning of installation, the piles moved down into the clay layers quite far due to their own weights so that pile driving started at about 19 m penetration. The soil parameters for the upper till and sand layers were estimated after the method of Stevens et al. (1982). Figures 7 and 8 show the results of the pile driving processes and the driveability based on the method of ICP-18, Jardine et al., 2018).

Again, ENTHRU calculated with simulations were adjusted to the measured energy at the pile top and calculated as well as measured blow counts are opposed.

Varieties in relevant parameters of equations 6a and 6b were considered in terms of the factorization of q_c (q_t) which ranges from 0.4 to 0.6. The interface friction angle was estimated so that δ'_{ult} was taken to 28° and 30° according to previous experiences.

As a result, the pile driving process could be simulated quite well at location II of a platform based on above mentioned input parameters. Blow counts, SRD and stresses show good agreement within the lower chalk formation layer (starting from about 47 m) whereas slightly too high blow counts and SRD were found in the chalk above.

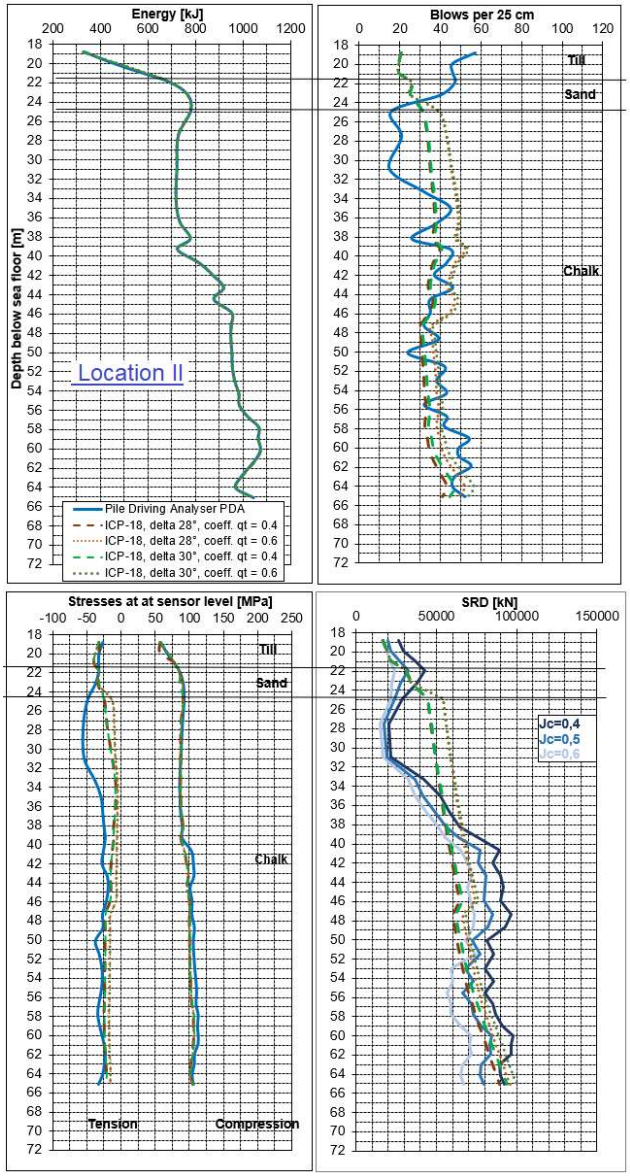

Fig. 7. Location II: Comparison of results from recorded hammer data, measuring data of dynamic pile test and driveability analyses (energy, blows per 25 cm penetration, pile stresses, SRD).

At location I of the platform larger deviations occur. The reason for that is supposed to arise from the simplification (constant value) in q_c for large depth intervals but requires further assessment.

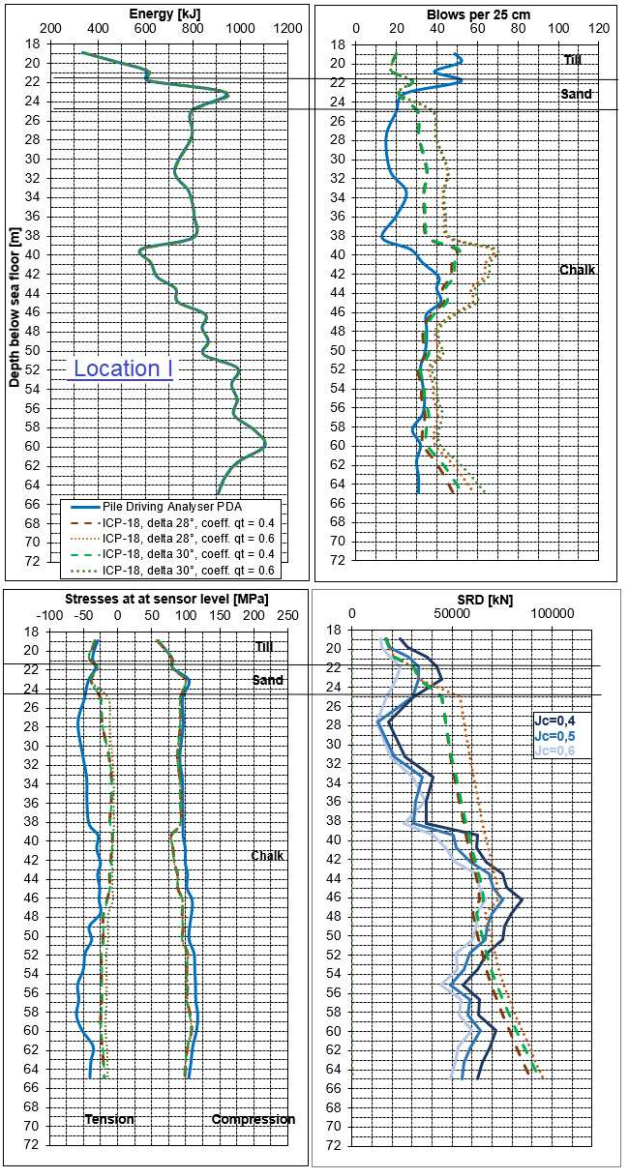

Fig. 8. Location I: Comparison of results from recorded hammer data, measuring data of dynamic pile test and driveability analyses (energy, blows per 25 cm penetration, pile stresses, SRD).

4.4 Driveability and results in soils, North Sea project – Vibratory driving

Results of vibratory driveability predictions at sandy locations 1 and 2 for a North Sea project are shown in Figures 9 and 10. To indicate a variation in driving best and higher estimates in soil resistances according to (Holeyman and Whenham, 2017) as well as a range of vibration frequencies of 15 Hz (900 RPM) and 20 Hz (1200 RPM) were chosen. Based on the ratio of eccentric moment and the dynamic mass (vibration parts of the vibrator + pile + clamps) times the squared angular frequency a vibration amplitude of about 17 m/s² and 30 m/s² in acceleration was found, respectively. The vibration frequencies are kept unchanged during the driving simulations although a slight change in frequency with depth levels is to be expected during installation.

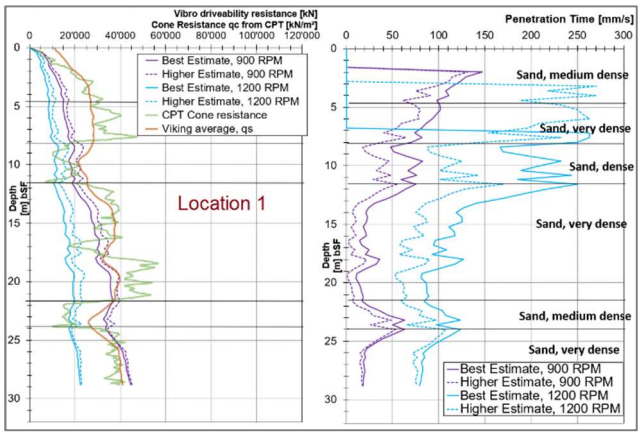

Fig. 9. Location 1 left: Vibro driveability resistance (blue and violet) with CPT data qc (green), Viking average qs (orange), Location 1 right: Penetration time (blue and violet).

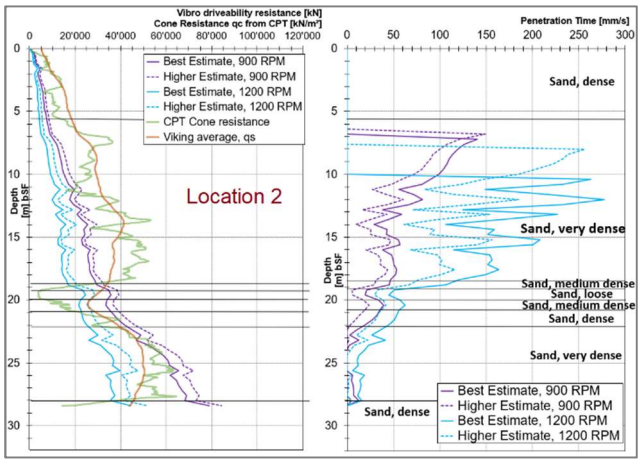

Fig. 10. Location 2 left: Vibro driveability resistance (blue and violet) with CPT data qc (green), Viking average qs (orange), Location 2 right: Penetration time (blue and violet).

While at location 1 vibratory driving is theoretically successful refusal may occur at location 2 at a depth of about 24 m for almost all variations. Obviously, this is the case because higher q_c values of almost 60 MPa at larger depth were found at location 2 compared to those at location 1 having an influence on power consumption of the vibrator.

Refusal is defined here as a certain limiting rate of penetration but no strict default. (Rausche, 2002) summarised values of 6,2 mm/s or 8 mm/s suggested by several authors but even 1 mm/s may be acceptable.

To calibrate present vibratory driveability the need of real measuring data is indispensable and further analysis will be undertaken.

5 CONCLUSIONS

This paper presented a link between theoretical driving simulations and real driving processes in a way that energies proved at driveability analyses had been calibrated at energies gained from measurement data. The goal of the study was to verify available SRD models whereas corresponding soil parameters (quake, damping) were set as usual experienced values.

Essential results of comparison could be summarised as follows:

- Real impact driving processes in soils could be retraced well based on the SRD methods. Best agreement in depth dependent blow counts development and resistances was identified with Alm & Hamres' method (Alm and Hamre, 2001), Schneider and Harmon, 2002).
- By using Stevens' method (Stevens et al., 1982) simulation result were achieved that differed considerably from the measurements at driving depth in particular next to the bottom end.
- For variable solid rock (chalk) the method of ICP-18, (Jardine et al., 2018) showed acceptable curve analogy versus measured data. Since no reliable CPT data were available an estimation of q_c based on soil samples was applied introducing constant values over the relevant depth intervals. This may be the reason for deviations within the lower chalk.
- Simulations of vibratory driving using Hypervib I model (Holeyman and Whenham, 2017) led to promising results and possibly successful installation for the analysed soil types. Real measuring data for calibration is not available yet. Vibration frequencies of 15 Hz and 20 Hz were applied both from the beginning right to the final penetration depth. A change in frequency with depth levels is to be expected during installations. (Massarsch, 2017) recommended to start driving at high frequencies achieving a high penetration rate in the beginning and lowering the frequency down to system resonance to cause soil densification at final penetration depth.

One main aspect in accordance with driveability is the acquisition of soil characteristic. Most current methods use data of cone penetration tests (CPT) in which variations in properties with depth can be distinguished. If no real measuring data is available like it is the case for driveability analyses prior to pile installation then an appropriate application of energy from hammer to pile must be chosen.

Continuous enhancement of a data base in junction with further recalculation of driving processes can serve as validation of gathered findings.

6 REFERENCES

1) Alm, T. and Hamre, L. (2001): Soil model for pile driveability prediction based on CPT interpretations, *International Conference on Soil Mechanics and Geotechnical Engineering,* Balkema, CONF 15, Vol. 2, pp. 1297-1302.

2) American Petroleum Institute (2000) incl. supplements (2007): Recommended Practice for Planning, Designing and Constructing Fixed Offshore Platforms - Working Stress Design, API-RP 2A-WSD.

3) Buckley, R.M., Jardine. R.J., Kontoe, S., Barbosa, P. and Schroeder, F.C. (2019): The design of axially loaded piles in chalk, *Proceedings of the XVII European Conference on Soil Mechanics and Geotechnical Engineering,* 10.32075/17ECSMGE-2019-0161, Reykjavik.

4) Buckley, R.M., Kontoe, S., Jardine, R.J., Barbosa, P. and Schroeder, F.C. (2020): Pile driveability in low-to-medium density chalk, *Canadian Geotechnical Journal 58*, 10.1139/cgj-2019-0703.

5) Chow, F. C., Jardine, R.J., Brucy, F. and Nauroy J.F. (1998): Effects of time on capacity of pipe piles in dense marine sands, *Journal of Geotechnical and Geoenvironmental Engineering.* Vol. 124, pp. 254-264.

6) GRL Engineers Inc. (2010): GRLWEAP, *Background Report,* Version 2010, Cleveland Ohio

7) Holeyman, A. and Whenham, V. (2017): Critical Review of the Hypervib1 Model to Assess Pile Vibro-Drivability, *Geotech Geol Eng 35,* pp. 1933-1951, 10.1007/s10706-012-9527-0.

8) Huybrechts, N., Legrand, Chr. and Holeyman, A. (2002): Drivability prediction of vibrated steel piles, *Proceedings of the International Conference on Vibratory Pile Driving and Deep Soil Compaction,* TRANSVIB2002, Balkema, pp.89-97.

9) IHC Hydrohammer B.V. (2013): Data sheet IHC S-1200 and IHC S-1800.

10) Jardine, R.J., Buckley. R.M., Kontoe, S., Barbosa, P. and Schroeder, F.C. (2018): Behaviour of piles driven in chalk, *Engineering in Chalk, Proceedings of the Chalk 2018 Conference,* London, pp. 33-51, 10.1680/eiccf.64072.033.

11) Massarsch, K.R., Fellenius, B.H. and Bodare, A. (2017): Fundamentals of the vibratory driving of piles and sheet piles, *Geotechnik 40*, Heft 2, Ernst & Sohn Verlag Berlin, S. 126-141, 10.1002/gete.201600018.

12) Maynard, A.W., Hamre, L., Butterworth, D. and Davison, F. (2018): improved Pile Installation Predictions for Monopiles, *Proceedings of the 10th International Conference on the Application of Stress Wave Theory to Piles,* San Diego, California (USA), pp. 426-449.

13) Schneider, J.A. and Harmon, I.A. (2010): Analyzing Drivability of Open Ended Piles in Very Dense Sands, *Deep Foundation Institute Journal*, Vol. 4, No. 1, pp.32-44.

14) Skov, R. and Denver, H. (1988): Time dependence of bearing capacity of piles, *Proceedings of the 3rd International Conference on the Application of Stress-Wave Theory to Piles*, Ottawa, Canada, pp. 25-27.

15) Smith, E.A.L. (1960): Pile Driving Analysis By The Wave Equation, *American Society of Civil Engineers, Journal of the Soil Mechanics and Foundation Engineering Division*, Vol. 86, Houston, Texas, pp.35-61.

16) Soares, M.M, Matos, S.F.D. and de Mello, J.R.C. (1984): Pile driveability study, pile driving measurements, *Proceedings of the 2nd International Conference on the Application of Stress-Wave Theory to Piles,* Stockholm, Sweden, pp. 64-71.

17) Stevens, R., Wiltsie, E.A. and Turton, T.H. (1982): Evaluating Pile Drivability for Hard Clay, Very Dense Sand, and Rock, *Proceedings of the 14th Annual Offshore Technology Conference,* Houston, Texas, Paper No. 4205.

18) Rausche, F. (2002): Modelling of vibratory pile driving, *Proceedings of the International Conference on Vibratory Pile Driving and Deep Soil Compaction,* TRANSVIB2002, Balkema, pp. 21-32.

19) Rausche, F., Liang, L., Allin R.C. and Rancman D. (2004): Applications And Correlations Of The Wave Equation Analysis Program GRLWEAP, *Proceedings of the 7th International Conference on the Application of Stress Wave Theory to Piles,* Malaysia, pp. 107-123.

20) Rausche, F., Likins, G. and Klingmüller, O. (2011): Auswertung dynamischer Messungen an großen offenen Stahlrohrpfählen, *Mitteilung des Instituts für Grundbau und Bodenmechanik*, Technische Universität Braunschweig, Heft Nr. 94, S. 491-507.

21) Viking, K. (2002): Vibro-driveability, a field study of vibratory driven sheet piles in non-cohesive soils, *PhD thesis*, Division of Soil and Rock Mechanics, Royal Institute of Technology, Stockholm, Sweden.

22) Webster, S. and Robinson, B. (2013): Driveability Analysis Techniques for Offshore Pile Installations, *Proceedings of the ASME 2013 32nd International Conference on Ocean, Offshore and Arctic Engineering,* OMAE 2013-11608, Nantes, France.